European Polymer Journal 141 (2020) 110075

Contents lists available at ScienceDirect

European Polymer Journal

journal homepage: www.elsevier.com/locate/europolj

Poly(methyl ethylene phosphate) hydrogels: Degradable and cell-repellent alternatives to PEG-hydrogels

Hisaschi T. Tee[a], Romina Zipp[b], Kaloian Koynov[a], Wolfgang Tremel[b], Frederik R. Wurm[c,*]

[a] Max-Planck-Institut für Polymerforschung, Ackermannweg 10, 55128 Mainz, Germany
[b] Institut für Anorganische und Analytische Chemie, Johannes Gutenberg- Universität Mainz, Mainz, Germany
[c] Sustainable Polymer Chemistry Group, MESA+ Institute for Nanotechnology, Faculty of Science and Technology, Universiteit Twente, PO Box 217, 7500 AE Enschede, the Netherlands[1]

ARTICLE INFO

Keywords:
Poly(ethylene glycol)
Hydrogel
Polyphosphoester
Phosphorus
Stealth effect

ABSTRACT

A degradable and water-soluble polyphosphoester (PPE), namely poly(methyl ethylene phosphate)-dimethacrylate (PMEP-DMA), was synthesized and crosslinked by UV irradiation to prepare PPE-hydrogels. Hydrogels with 10 and 15 wt% of PMEP were prepared after UV-irradiation with an additional 0.2 wt% of photoinitiator. The colorless and transparent PPE hydrogels were studied for their swelling and water uptake. The rheological analysis demonstrated their viscoelastic behavior. The PPE hydrogels were compared to poly(ethylene glycol) (PEG) hydrogels prepared from PEG-macromonomers of similar degrees of polymerization. Hydrolysis experiments proved a successful disintegration of the PPE hydrogels compared to PEG analogs; a faster weight loss for the hydrogels with 10 wt% of PMEP compared to the 15 wt% hydrogels was detected. NMR spectroscopy further proved the release of soluble PPEs from the network and the formation of phosphoric acid diesters during the hydrolysis. Finally, the cytotoxicity with the MG-63 osteoblast cell lines and proved low cell toxicity from the hydrogels with no significant cell adherence towards the gels similar to PEG-based hydrogels. In summary, this work proves PMEP-hydrogels as degradable alternatives to PEG-hydrogels with similar hydrophilicity and low cell adhesion, which might be used in further tissue engineering and to prevent polymer accumulation.

1. Introduction

Poly(ethylene glycol) (PEG) hydrogels have proven great promises for biomedical applications as matrices for controlled release of therapeutics or as scaffolds for promoting tissue regeneration [1–4]. These PEG hydrogels are non-cytotoxic, non-immunogenic, hydrophilic and they can mask the material from the host's immune system, which renders them a great material for regenerative medicine applications [2]. However, PEG hydrogels have a low additional functionality, given that the functionalization of the polymer is limited to the hydroxyl chain end(s) [4,5]. In addition, degradation of the hydrogel network is mostly achieved via ester bonds attached to the chain ends and used for crosslinking, e.g. by methacrylic acid esters [6]. The methacrylate esters in the PEG hydrogel can hydrolyze; however, the non-degradable PEG chains need to be washed out or can induce bioaccumulation in the tissue [7,8]. Degradable PEG-based hydrogels were reported, relying on block-copolymers with degradable poly(lactic acid) (PLA) segments [9–12]. The introduction of PLA to form degradable hydrogels has found many successful applications, however, this type of polymer composition can have drawbacks such as potential inflammation caused by acidic degradation products from lactic acid and poly(acrylic acid), protein denaturation [12–14]. Another approach to degradable but also hydrophilic PEG hydrogels utilized multiarm PEG-amine for the cross-linking of active-ester-containing PEG derivates [15]. Due to the amine reaction during the cross-linking, the covalent binding of encapsulated proteins to the polymer network can occur, which limits its applications.

Phosphorus-containing polymers, especially polyphosphoesters (PPEs), are materials that have attracted a lot of attention for biomedical applications as they fulfill many of the desired properties [16,17]: Water-soluble PPEs have a similar "stealth effect" and low cell adhesion as PEG [18] and their physical properties can be controlled by the binding pattern around the phosphorus atom (e.g. phosphate or phosphonate) [19,20]. With the ester bonds in the backbone, PPEs are

* Corresponding author at: Sustainable Polymer Chemistry Group, MESA+ Institute for Nanotechnology, Faculty of Science and Technology, Universiteit Twente, PO Box 217, 7500 AE Enschede, the Netherlands
E-mail address: frederik.wurm@utwente.nl (F.R. Wurm).
[1] https://www.utwente.nl/en/tnw/spc/.

https://doi.org/10.1016/j.eurpolymj.2020.110075
Received 6 August 2020; Received in revised form 4 September 2020; Accepted 29 September 2020
Available online 15 October 2020

hydrolytically degradable and the pentavalent phosphorus atom allows a high structural and chemical versatility. Water-soluble PPEs can be prepared by the ring-opening polymerization of cyclic phosphoester monomers by organo- or metal-catalysis [17,21–25]. PPEs were studied as matrices for hydrogels previously, but only copolymers or post-polymerization modification was used for their preparation [26–28]. Besides, PPEs have been combined with polyethylene glycol (PEG), polysaccharides, or catechols to prepare degradable hydrogels. [29–31].

Herein, we report polyphosphoester hydrogels that exhibit the desired cell-repellent properties and also being degradable and potentially chemically tunable. Poly(methyl ethylene phosphate) (PMEP) with its high hydrophilicity was used as a PEG analog. It was synthesized by the ring-opening polymerization (ROP) of the five-membered 2-methoxy-1,3,2-dioxaphospholane 2-oxide (MEP) heterocycle. This polymer has been used in water-soluble PPEs since decades, however, to our knowledge, it has never been used for the preparation of hydrogels. Various crosslinking strategies mainly relying on free radical polymerization had been developed for the preparation of hydrogels for biomedical applications, including tissue engineering scaffolds, wound dressing, drug delivery, artificial blood vessels, tissue regeneration, etc. [32–34]. Herein, we used UV-crosslinking for the hydrogel formations by introduction of two methacrylate end groups by terminating the ROP with 2-isocyanatoethyl methacrylate. The hydrogels were then prepared by UV irradiation in the presence of a photoinitiator (Irgacure 2959) in aqueous solution of the polymers in analogy to conventionally used PEG-methacrylates.

In general, PPE hydrogels might be a suitable alternative for PEG-hydrogels, if additional biodegradation is required in biomedical applications or further tuning of hydrophilicity and functionality is needed.

2. Materials

All solvents and chemicals were purchased from Sigma Aldrich, Acros Organics, or Fluka and used as received unless otherwise stated. DBU was distilled from calcium hydride and stored over molecular sieves (4 Å) under argon before use. Dry solvents were purchased from Acros Organics or Sigma Aldrich and stored with a septum and over molecular sieves. Deuterated solvents were purchased from Sigma Aldrich and used as received. 2-Chloro-1,3,2-dioxaphospholane 2-oxide (COP), 2-Hydroxy-4′-(2-hydroxyethoxy)-2-methylpropiophenone, and DPBS - Dulbecco's Phosphate-Buffered Saline (DPBS) and other reagents were bought from Sigma Aldrich.

2.1. Instrumentation and characterization techniques

Size exclusion chromatography (SEC) measurements were performed in DMF (containing 1 g L^{-1} of lithium bromide as an additive) at 60 °C and a flow rate of 1 mL min^{-1} with a PSS SECurity as an integrated instrument, including a set of 3 PSS GRAM columns (porosity of 100 Å and 1000 Å) and a refractive index (RI) Detector. Calibration was carried out using polyethylene glycol standards provided by Polymer Standards Service. For nuclear magnetic resonance analysis ^{1}H, ^{13}C, and ^{31}P NMR spectra of the monomers and polymers were recorded on a Bruker AVANCE III 300, 500 or 700 MHz spectrometer. All spectra were referenced internally to residual proton signals of the deuterated solvent. The high-pressure liquid chromatography (HPLC) measurements were performed on an Agilent Technologies Series 1200 setup equipped with a UV detector and an ELSD detector 385-LC (both Agilent Technologies, Santa Clara, USA). The analysis of polymers was conducted using a Macherey-Nagel MN HD8 column 125/4/5 µm equipped with a 5–3 precolumn (Merck Chemicals GmbH, Darmstadt, Germany) and an eluent gradient from MeOH/water + 0.1% TFA 40/60% to 100/0% in 10 min. For each measurement, 10 µL of sample volume was injected and kept at 37 °C throughout the measurement The thermal properties of the synthesized polymers have been measured by differential scanning calorimetry (DSC) on a Mettler Toledo DSC 823 calorimeter. Three scanning cycles of heating − cooling were performed in an N_2 atmosphere with a heating and cooling rate of 10 °C min^{-1}. TGA was measured on a Mettler Toledo ThermoSTAR TGA/SDTA 851-Thermowaage in a nitrogen atmosphere. The heating rate was 10 °C min^{-1} in a range of temperatures between 25 and 600–900 °C. FTIR spectra were recorded in transmission mode accomplished with a Bruker Tensor II (Platinum ATR). Rheology experiments were performed on an Advanced Rheometric Expansion System (ARES, Rheometric Scientific). Plate-plate geometry was used with plate diameters of 25 mm. Oscillatory shear deformation was applied under conditions of controlled deformation amplitude. Strain sweeping at a constant frequency of 1 rad/s was first performed (from 10^{-3}% to 10^{2}%) for the individual hydrogels. Then the strain was fixed at a selected value in the range of linear viscoelastic response and the frequency sweeping was performed from 10^{-1} to 10^{2} rad/s. LogP values were calculated via the free online tool on www.molinspiration.com with 92 repeating units for PEG and 32 repeating units for PMEP. SEM investigations were performed by using an LEO 1530 GEMINI. The characterizations were carried out by applying the low-voltage approach. The lyophilized gels were deposited on conductive carbon tape.

2.2. Experimental

2.2.1. 2-Methoxy-2-oxo-1,3,2-dioxaphospholane (MEP) (**M1**) [35]

A flame-dried 1000 mL three-neck flask, equipped with a dropping funnel, was charged with 2 chloro-2-oxo-1,3,2-dioxaphospholane (50 g, 0.35 mol) dissolved in dry THF (300 mL). A solution of dry methanol (11.24 g, 0.35 mol) and dry triethylamine (35.42 g, 0.35 mol) in dry THF (45 mL) was added dropwise to the stirring solution of COP at −20 °C under an argon atmosphere. During the reaction, hydrogen chloride was formed and precipitated as triethylammonium hydrochloride. The reaction was stirred at 4 °C overnight. The salt was removed by filtration and the filtrate concentrated *in vacuo*. The residue was purified by distillation at reduced pressure to give a fraction at 89–97 °C/0.001 mbar, obtaining the clear, colorless, liquid product MEP (37.21 g, 0.27 mol, yield: 77%). ^{1}H NMR (500 MHz, $CDCl_3$, 298 K): δ = 4.43 (m, 4H), 3.71 (d, 3H) ppm. $^{13}C\{H\}$ NMR (125 MHz, $CDCl_3$, 298 K): δ 66.57, 54.72. ^{13}C NMR (75 MHz, $CDCl_3$, 298 K) δ = 66.19, 66.16, 54.93, 54.84 ppm.$^{31}P\{H\}$ NMR (202 MHz, DMSO-d_6, 298 K): δ = 17.89 ppm.

2.2.2. Polymerization to PMEP-DMA (**P1-DMA**) [36]

N-cyclohexyl-*N*′-(3,5-bis(trifluoromethyl)phenyl)thiourea (TU) was synthesized according to the literature procedure [37]. TU and the initiator PEG 400 were freeze-dried with benzene prior use. MEP (5.26 g, $7.2{\cdot}10^{-3}$ mol), TU (1.41 g, $13.73{\cdot}10^{-3}$ mol), PEG 400 (0.55 g, $1.37{\cdot}10^{-3}$ mol) and 0.56 mL dry dichloromethane were introduced into a 100 mL flame dried Schlenk tube to give a total reaction concentration of 4 mol/L MEP in dichloromethane. The polymerization was initiated by rapid addition of 2.05 mL DBU (2.09 g, $13.7{\cdot}10^{-3}$ mol) to the stirring solution with a syringe at 0 °C. The polymerization was terminated after 1 h by excess addition of 2-isocyanatoethyl methacrylate (4.27 g, $27.5{\cdot}10^{-3}$ mol). The polymer was precipitated twice from dichloromethane into ice-cold ethyl acetate and once into ice-cold diethyl ether. 0.067 mol% hydroquinone was added, the mixture dissolved in deionized water and then freeze-dried. The polymer was obtained after freeze-drying in quantitative yield. ^{1}H NMR (300 MHz, $CDCl_3$, 298 K) δ = 6.11 (s, 2H), 5.56 (s, 2H), 4.43–4.11 (m, 327H), 3.93–3.69 (m, 239H), 3.65–3.56 (m, 36H), 1.91 (s, 1H) ppm. $^{13}C\{H\}$ NMR (75 MHz, $CDCl_3$, 298 K) δ = 70.53, 66.41, 66.33, 66.24, 54.70, 54.62 ppm. $^{31}P\{H\}$ NMR (121 MHz, DMSO-d_6, 298 K) δ = 1.10, −0.20, −1.52 ppm.

2.2.3. PEG(4,000)-DMA and PEG(10,000)-DMA (**P2-DMA**)

PEG-DMA was synthesized according to literature [38]. Briefly, PEG

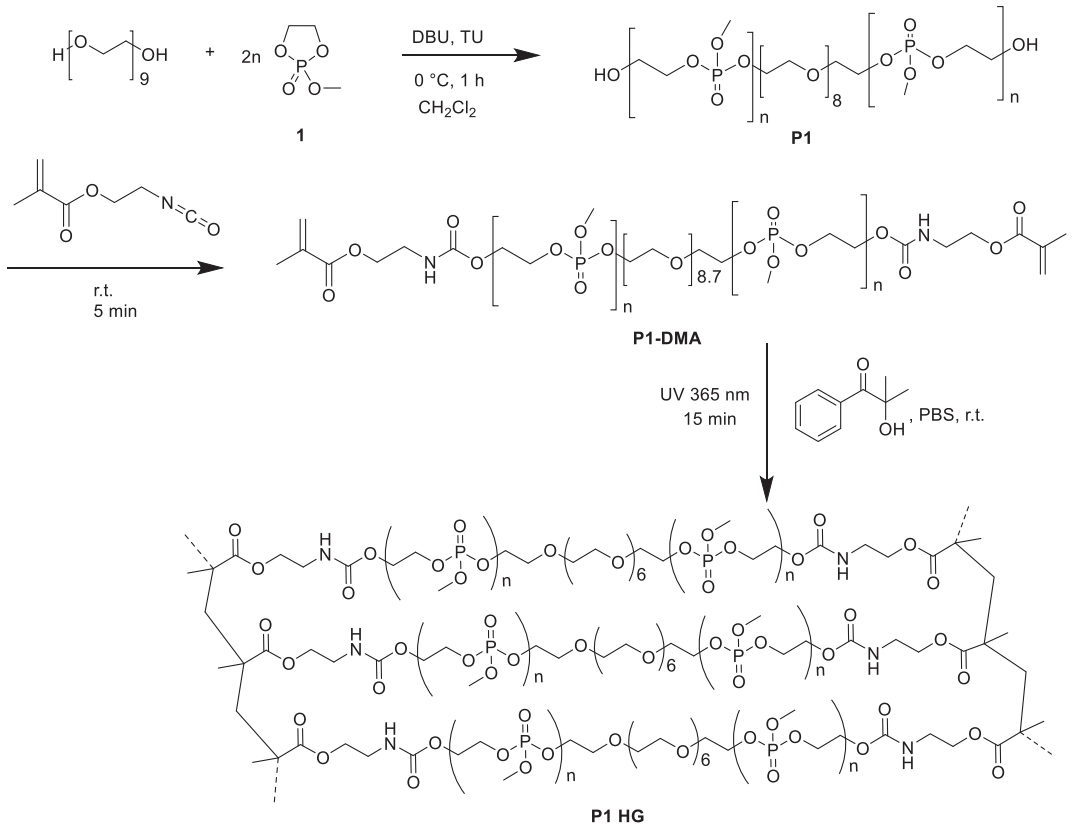

Scheme 1. Polymerization of MEP (1) and subsequent preparation of hydrogels.

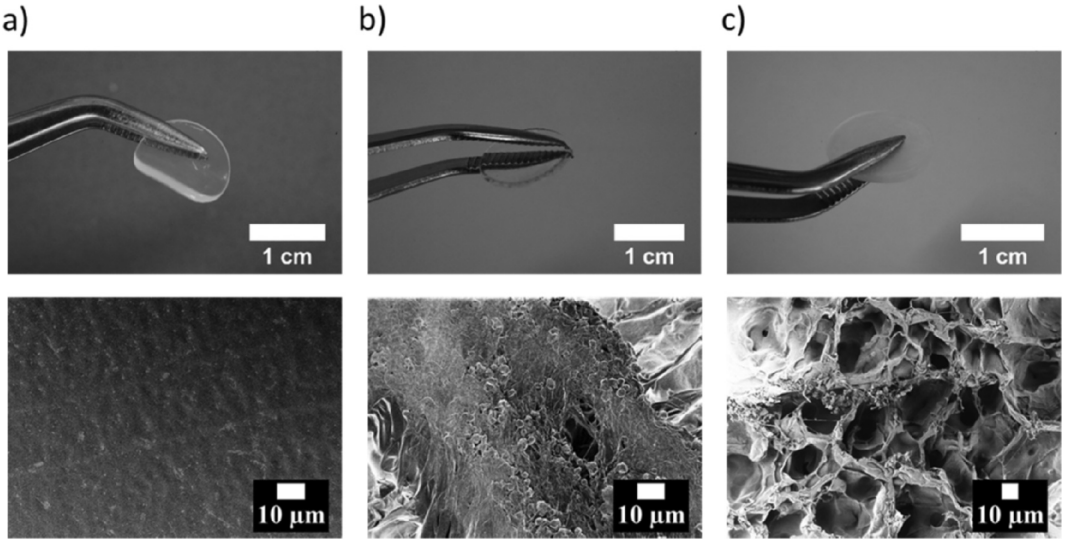

Fig. 1. Top: photos of the hydrogels after polymerization and SEM images of lyophilized hydrogels. (a) 15 wt% PMEP HG, (b) 15 wt% PEG(4,000) HG and (c) 15 wt% PEG(10,000) HG.

(5 g, $1.25{\cdot}10^{-3}$ mol(4,000) or $0.50{\cdot}10^{-3}$ mol(10,000)) was added to a solution of dibutyltin dilaurate (DBTD) (2 drops) and 15 mL dry dichloromethane over freshly activated molecular sieves (ca. 6 g). The reaction was then stirred for 4 days at room temperature. The solution was precipitated twice from dichloromethane into diethyl ether. The product was isolated by filtration as a colorless powder. The PEG-DMA was dissolved in deionized water, 0.1 wt% hydroquinone was added and the solution was freeze-dried to give the pure product in yields typically above 90%.

PEG(4,000)-DMA: ^{1}H NMR (300 MHz, $CDCl_3$, 298 K) δ = 6.10 (s, 2H), 5.58 (s, 2H), 5.25–5.05 (m, 2H), 4.46–4.10 (m, 4H), 4.01–3.44 (m, 364H), 3.44–3.19 (m, 4H) 1.93 (s, 6H) ppm. ^{13}C NMR (75 MHz, $CDCl_3$, 298 K) δ = 126.02, 70.57, 69.57, 18.31 ppm. PEG(10,000)-DMA: ^{1}H NMR (300 MHz, $CDCl_3$, 298 K) δ = 6.12 (s, 2H), 5.60 (s, 2H), 5.18–5.08 (m, 2H), 4.31–4.14 (m, 4H) 3.94–3.46 (m, 908H), 3.45–3.31 (m, 4H), 1.94 (s, 6H) ppm. ^{13}C NMR (75 MHz, $CDCl_3$, 298 K) δ = 118.16, 70.57 ppm.

2.2.4. Hydrogel formation by photopolymerization

For the preparation of PMEP hydrogels, 500 µL of a 10 or 15% (w/v) solution of PMEP-DMA in DPBS was mixed with 10 µL of the photoinitiator 2-hydroxy-4′-(2-hydroxyethoxy)-2-methylpropiophenone used

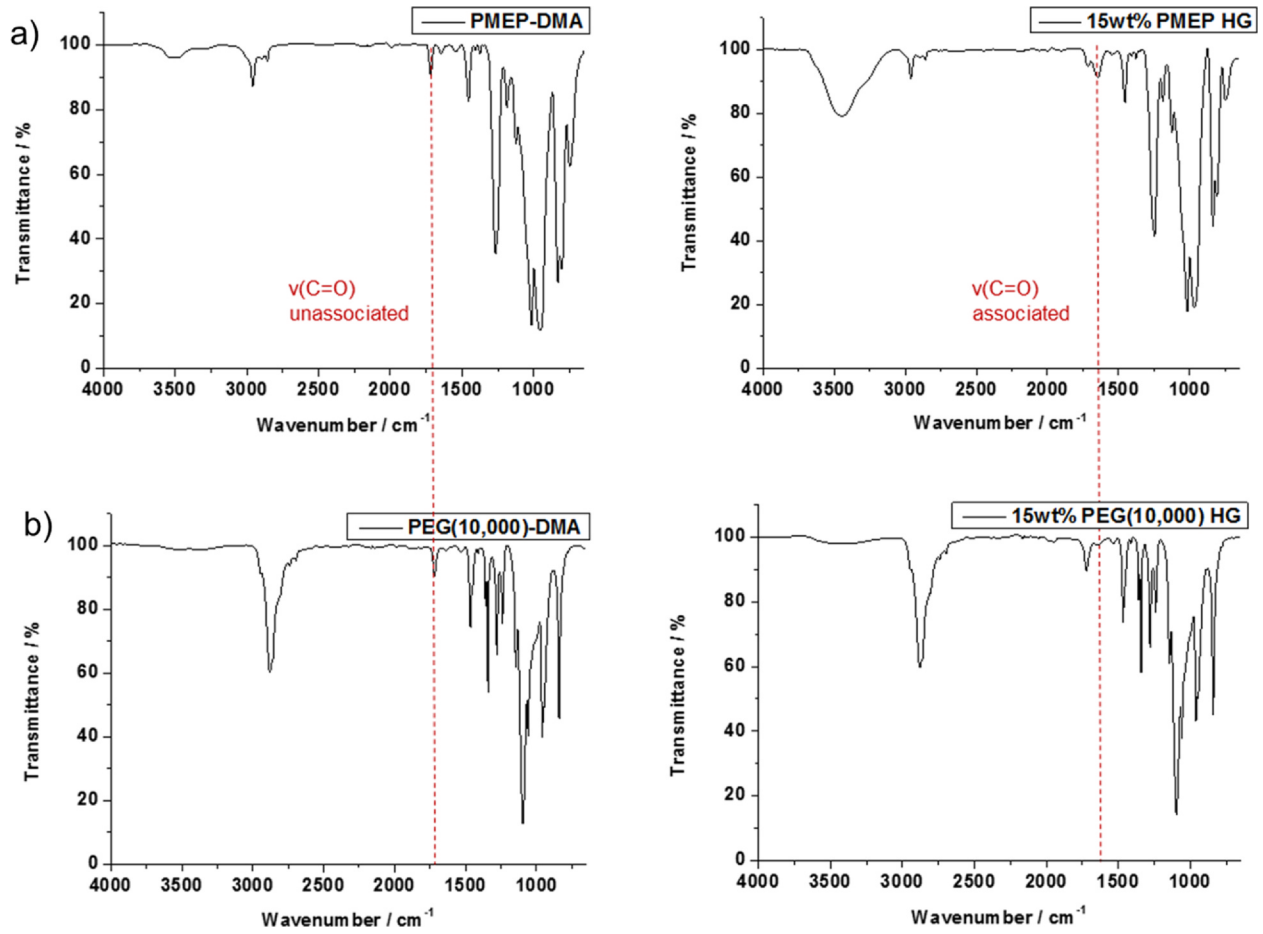

Fig. 2. IR spectra of (a) PMEP-DMA precursor and 15 w% PMEP-hydrogel. (b) PEG(10,000)-DMA precursor and 15 w% PEG(10,000) hydrogel.

as 10% (w/v) solution in 70% ethanol (2 g of the initiator were dissolved in 20 mL 70% EtOH). 0.1 mL of the polymer-photoinitiator solution was transferred to a 48-well plate and the same volume of isopropanol was added to remove emerging air-bubbles and to suppress capillary effects. The polymerization of all hydrogels was initiated by 365 nm UV irradiation with a DC lamp directly placed on the well plate for 15 min. PMEP-DMA hydrogel for rheology was synthesized in a cylinder with a 26 mm diameter with 1.06 mL polymer solution and isopropanol. The PEG hydrogels were synthesized following the same protocol as the PMEP hydrogels. The hydrogels were washed three times with 1 mL deionized water at 150 rpm for 5 min before further tests.

2.2.5. Hydrolytic degradation of the hydrogels

The degradation of the hydrogels was conducted at 37 °C by immersing each gel (12 mm diameter) in 5 mL 0.1 M DPBS (pH 7.4) in closed 20 mL vials. The hydrogels were removed from the solution after predetermined time intervals, surface water was removed and the gels were freeze-dried. The weights of the lyophilized gels before (average weight of 3 samples) and after degradation were compared. For ^{31}P NMR degradation kinetics, a full 15 w% PMEP HG with 12 mm diameter was transferred into an NMR tube and 0.5 mL DPBS/D_2O 9:1 were added.

2.3. Determination of the swelling ratio

Hydrogels were immersed for 6 h and 26 h in DPBS or deionized water at room temperature. Then the mass swelling ratio of the swollen mass to the dry, lyophilized mass of polymer was calculated and compared. The swelling ratio Q was calculated by dividing the mass of the swollen gel after a certain time by the mass of the freshly synthesized and washed gel.

2.4. Cell culture

The human osteoblast cell line MG-63 (ATCC® CRL-1427®, LGC Promochem) was used and cultured in DMEM (high glucose, Sigma–Aldrich), 10% FBS (Sigma–Aldrich) + 2 mM Glutamax I (Gibco® Thermo Fisher Scientific) + 100 U/100 µg/mL Penicillin/Streptomycin (Gibco Thermo Fisher Scientific).

2.5. Visualization and characterization of cell viability and proliferation

The biocompatibility upon exposure to vaterite was evaluated with MG-63 plated in sterile 12-well cell culture plates (Greiner bio-one Cellstar). Cells were seeded at 100,000 MG-63 cells per well. The cells were evaluated optically using fluorescence microscopy after 24 h, 72 h and 7 days. The cell culture medium was replaced on Days 3 and 6, respectively. The studies were carried out as double determinations. Cell cultures were analyzed for viability and proliferation by fluorescence microscopy (BZ-9000E BIOREVO, Keyence). Calcein-AM was used for detecting the viable cells by adding 10 µM Calcein AM (Thermo Fisher Scientific) into the culture medium and incubating for 10 min at 37 °C [39]. Calcein - AM is converted to strong green fluorescent when taken up by viable cells after intra-cellular esterases remove the acetomethoxy (AM) group.

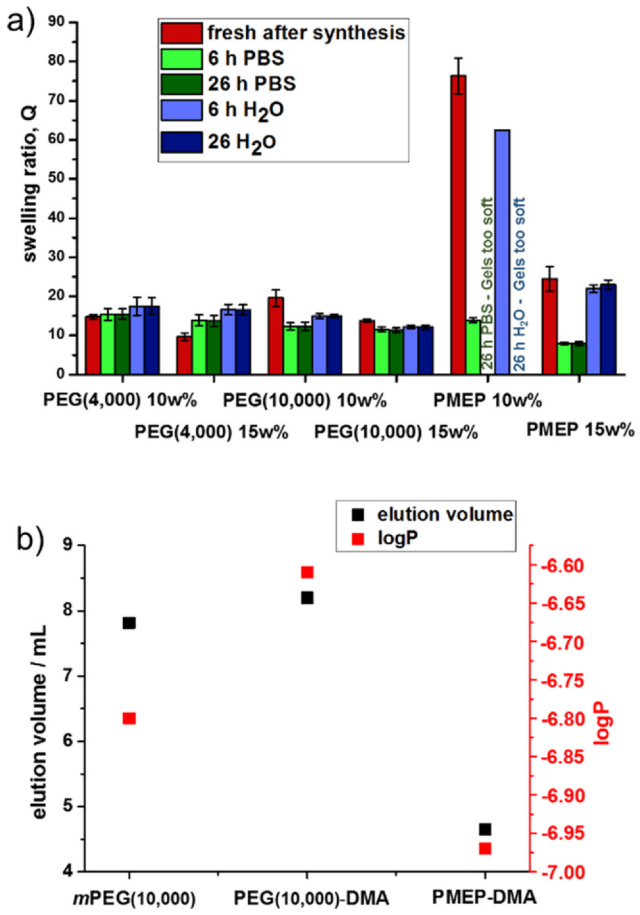

Fig. 3. (a) Swelling ratio of the hydrogels after 6 and 26 h equilibration in deionized water or 0.1 M PBS buffer. (b) Determination of the hydrophilicity of PMEP and PEG via reverse-phase HPLC (rpHPLC) and calculated logP-values.

3. Results and discussion

3.1. Polymer synthesis and hydrogel preparation

The crosslinkable PPE macromonomers were prepared by the anionic ring-opening polymerization of MEP (1) with a mixture of 1,8-diazabicyclo[5.4.0]undec-7-ene (DBU) and 1-(3,5-bis(trifluoromethyl) phenyl)-3-cyclohexylthiourea (TU) as catalyst/cocatalyst system. [40] PEG-diol of M_n = 400 g/mol was used as a difunctional initiator. The polymerization was conducted at 0 °C for 60 min and terminated by the addition of 2-isocyanatoethyl methacrylate to give the dimethacrylate-terminated PMEP-DMA as a colorless viscous liquid (Scheme 1, **P1**; $M_{n\,(NMR)}$ = 12,000 g/mol with 80 repeating units as determined by ^{1}H NMR, $M_{n(GPC)}$ = 5,700 g/mol and a molar mass dispersity of $Đ$ = 1.8 (from GPC)). The ^{1}H NMR spectra of **P1-DMA** exhibited the characteristic signal of the methylene groups in the backbone at 4.29–3.93 ppm and the methyl groups of the pendant side chain at 3.78–3.53 ppm. The signals of the initiator appeared at 3.57–3.46 ppm, while the resonances of the methacrylate double bonds were detected at 6.06 and 5.68 ppm, respectively. The ^{31}P NMR spectrum of **P1-DMA** showed the main backbone signal at −0.20 ppm and two additional smaller signals at 1.10 and −1.48 ppm for the end-groups (Fig. S2).

The hydrogels were prepared by UV irradiation (15 min at 365 nm) of a 10 or 15 wt% solution of PMEP-DMA in 0.1 M PBS buffer (pH 7.4) containing 0.2% of 2-hydroxy-4′-(2-hydroxyethoxy)-2-methylpropiophenone (Irgacure 2959, Scheme 1). UV irradiation of the PMEP-DMA solution in the presence of the water-soluble photoinitiator Irgacure 2959 photoinitiator produced benzoyl and α-substituted alkyl radicals that readily result in the crosslinking of the PPE [41]. After the irradiation time, clear, colorless and soft PMEP hydrogels were obtained (Fig. 1).

As comparison, we prepared two PEG hydrogels, using PEG diols (4,000 g/mol or 10,000 g/mol), which were functionalized with 2-isocyanatoethyl methacrylate and a catalytic amount of dibutyltin dilaurate (Synthesis is shown in Scheme S1, characterization data in Figs. S3–S5)). Crosslinking to the hydrogels was performed in the same way as for the PMEP hydrogels. Compared to the flexible, colorless, and transparent PMEP-HG, the obtained PEG-hydrogels were stiffer and slightly turbid, probably due to partly crystallization of PEG after lyophilization (Fig. 1). We expect the similar crosslinking densities for the PEG(4,000) hydrogel (DP_n = ca. 90) and the PMEP-based hydrogel (DP_n = ca. 80), due t similar degrees of polymerization, while the crosslinking density for the PEG(10,000)-based hydrogel is comparably lower due to a DP_n of ca. 220.

Characterization of the hydrogels. SEM is a typical technique used to visualize the interior hydrogel structure, however the pretreatment of the dehydration and/or fixation processes for SEM observation may alter the hydrogel morphology [42]. SEM images of lyophilized hydrogels show a strong difference between the morphology of PMEP and PEG hydrogels. While PMEP hydrogels showed a relatively smooth surface without any detectable mesh-structure (Fig. 1), PEG –based hydrogels exhibited the characteristic meshes of a three-dimensional polymer network. The difference in the visualized morphology after lyophilization by SEM can be explained by the different thermal properties of PEG and PMEP. As PMEP is a fully amorphous, low T_g-material, the mesh structure collapsed after freeze-drying. DSC measurements proved the fully amorphous structure of PMEP-DMA with a glass transition (T_g) of −39 °C, similar to other poly (alkyl ethylene phosphate)s [35]. PEG on the other hand is a solid, partly crystalline polymer with a T_m of 51 and 58 °C for PEG(4,000)-DMA and PEG(10,000)-DMA, respectively. This results in the retaining of the cellular structure after freeze-drying, while the PMEP-HGs no cellular structure can be visualized by SEM.

IR spectra of the PMEP-DMA or PEG-DMA precursors and the corresponding hydrogels prove the successful photopolymerization. For all soluble precursors and hydrogels absorption bands at 1730 cm^{-1} for the C = O group in the urethane linkage and at 1540 cm^{-1} for the NH-vibrations were identified. In the hydrogels, the intensity of the vibration band at 1700 cm^{-1} was increased, indicating the associated C = O groups in the urethane-linkages in the gel network. For the PMEP-DMA and the corresponding hydrogel in the region of 1350–1150 cm^{-1} the stretching vibration of the P = O group was detected. In the precursor, PMEP-DMA, the P = O stretching for unassociated P = O bonds was detected 1350 cm^{-1} (Fig. 2). The band for P = O stretching in the gels shifts to 1250 cm^{-1}, which is typical for associated P = O bonds and is due to hydrogen bonding of the phosphates with trapped water inside the gel. Both hydrogels showed a clear O-H vibration band at 3450 cm^{-1} resulting from residual water, trapped in the cross-linked polymer network. The PMEP-hydrogel had a significantly stronger signal for the O-H vibrations compared to the PEG-based hydrogel, which might be rationalized by the more efficient trapping of water in the amorphous hydrogel of PMEP during the drying process.

Swelling ratio. The swelling ratio of a hydrogel is an important value for various applications as it strongly influences the surface properties, mechanical properties, surface mobility as well as diffusion of solutes through the network [1]. The amount of water retained by the hydrogel depends on the structure of the polymer network itself and environmental conditions such as ionic strength, pH, and temperature of the aqueous solution in contact with the polymer [43]. Since the physical properties can be changed with hydration, the mass swelling ratio of the gels was investigated relative to polymer concentration and swelling time. Hydrogels were immersed into DPBS and deionized water at room temperature for 6 h or 26 h. Then, the mass swelling ratio of the swollen mass to the dry, lyophilized mass of polymer was calculated and compared (Fig. 4a). The swelling ratio Q was calculated

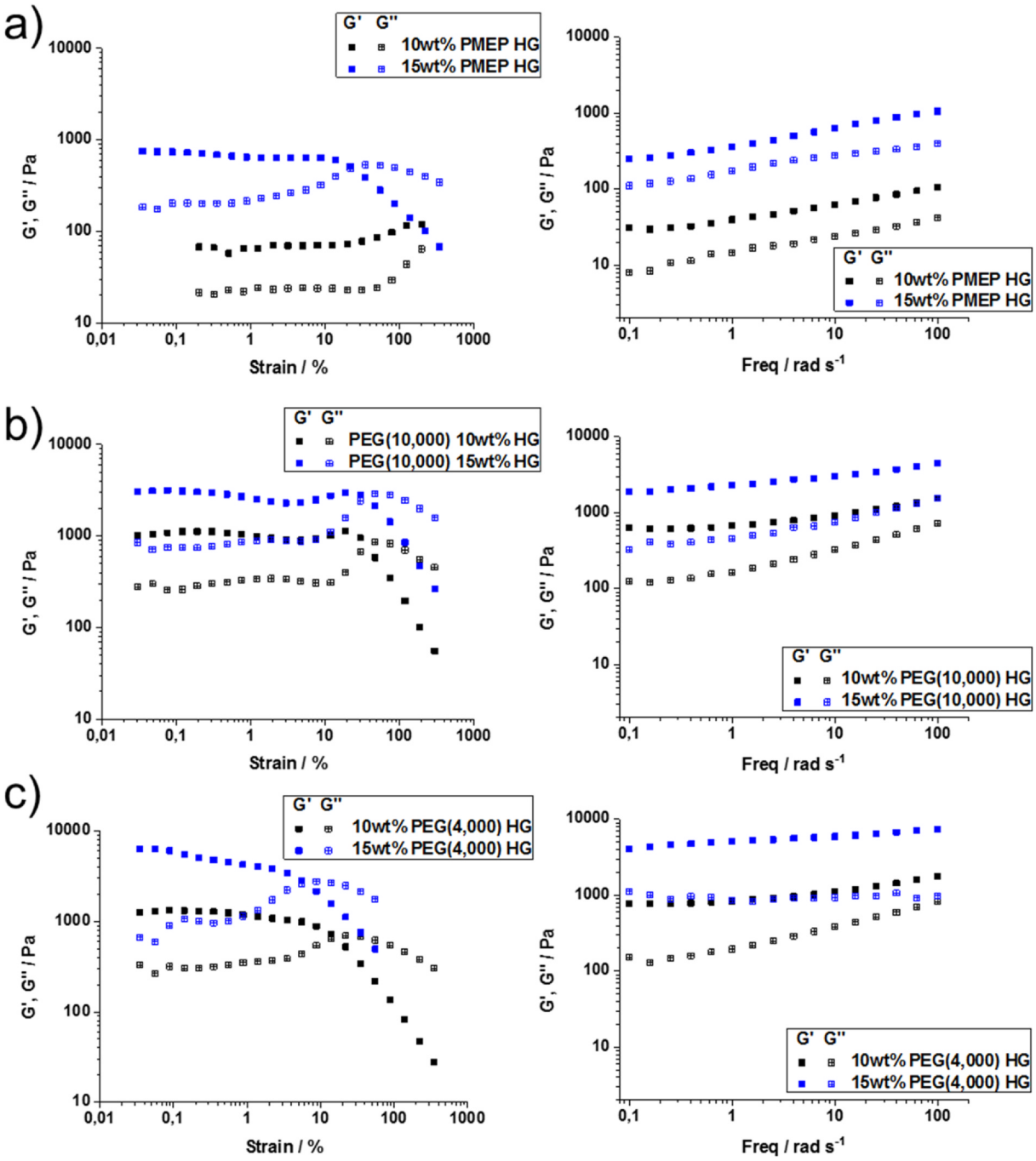

Fig. 4. Rheological characterization of (a) 10 and 15 wt% PMEP HGs, (b) 10 and 15 wt% PEG(4,000) HGs and (c) 10 and 15 wt% PEG(10,000) HGs by strain sweeps at fixed frequency (1 rad/s) and frequency sweeps at constant strain.

according to

$$Q = \frac{w_{gel,swell,time}}{w_{gel,dry}} \quad (1)$$

where $w_{gel,\ swell,\ time}$ is the swollen hydrogel after 6 h or 26 h and $w_{gel,\ dry}$ is the weight of the dried hydrogel.

When comparing both PEG hydrogels with PMEP hydrogels, the PEG gels exhibited a very similar swelling in DPBS and water. A slight increase in the swelling ratio seemed to occur for the 15 wt% PEG hydrogels after incubation compared to the "as prepared" gels. In the case of PMEP hydrogels, a significantly higher swelling ratio was calulated compared to the PEG-hydrogels for 10 wt% hydrogels directly after the synthesis or after immersing in the water for 6 h. If the 10 wt% PMEP-hydrogel was immersed into DPBS, the swelling ratio decreased to similar values as PEG-hydrogels, probably due to interactions with the salt ions in DPBS. For longer incubation times, the 10 wt%-PMEP-hydrogels became too soft and the swelling ratio could not be determined. The 15 wt% PMEP hydrogels proved to be mechanically more stable and exhibited a similar swelling after the crosslinking and after immersing them into pure water. The gels, incubated in DPBS proved a significantly lower swelling ratio, compared to the PEG hydrogels, probably attributed to stronger interactions of the polyphosphoester backbone with salt ions compared to the polyether backbone (Fig. 3a). The difference in the swelling ratios in pure water of PMEP-hydrogels compared to the PEG analogs might be rationalized also by the higher hydrophilicity of PMEP compared to PEG, which was confirmed by

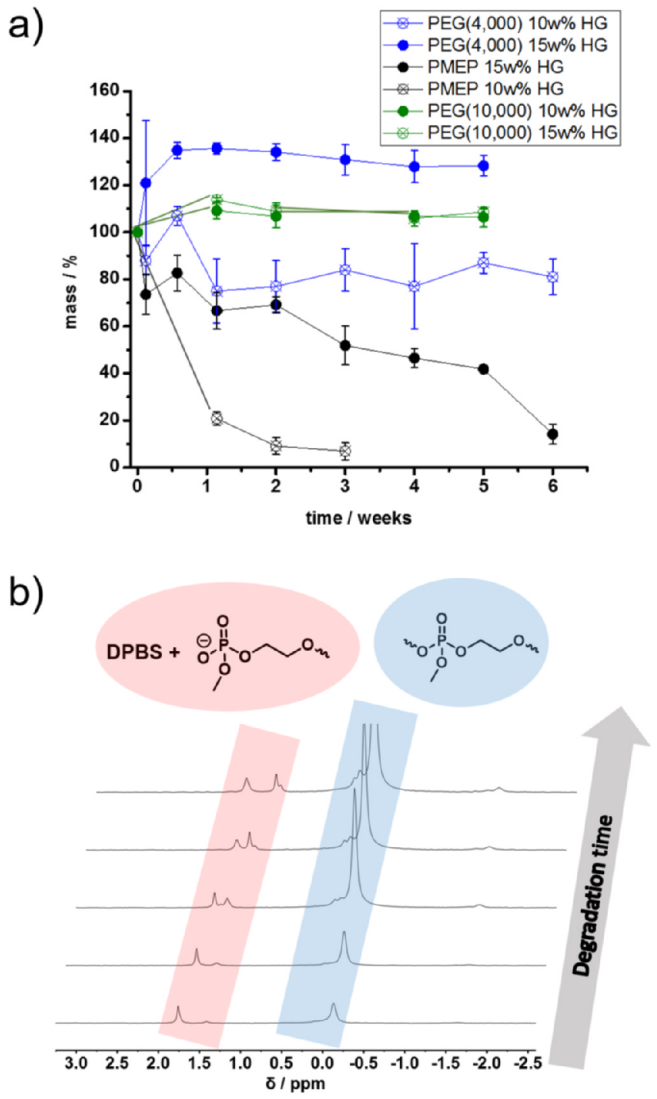

Fig. 5. Hydrolysis of hydrogels. (a) Mass change of hydrogels in 0.1 M PBS buffer at 37 °C. (b) ^{31}P NMR spectra (202 MHz, 298 K, 0.1 M DPBS/D_2O (9:1)) recorded within the degradation of PMEP HG at pH 7.4 after 0, 3, 8, 25 and 41 days.

calculation of the theoretical logP value or by the elution time via rpHPLC (Figs. 3b and S8). rpHPLC has been used previously to compare the hydrophilicity of polyphosphoesters (with variable side chains) to polyethylene glycol and found to be a straightforward tool to quantify and correlate to logP values [44].

Mechanical Properties. Mechanical properties of hydrogels are known to influence cell function and differentiation and thus are important for application on tissue engineering [45,46]. The mechanical properties of hydrogels are dependent on the cross-linking density, the swelling, ratio, which depend directly on the chemical structure of the polymers used for their preparation. Further, the polymer concentration of the hydrogels determine their mechanical properties and swelling behavior [47]. To investigate the mechanical properties of the PPE hydrogels, oscillatory shear rheology was used and the storage (G′, elastic component) and loss moduli (G″, viscous component) of the gels as a function of either strain or frequency were measured. The profiles of all 10 and 15 wt% hydrogels are summarized in Fig. 4: the strain sweeps indicate that linear plateaus are clearly present for both the viscosity-curve and elasticity-curve of all gels. The sharp bend of the G' curve after the yield stress indicates a brittle fracture behavior of the gels due to uneven breaking under shear. With G' > G'' in the linear zone and the peak of G'' with increasing shear, the crosslinking of the hydrogels was underlined, with first micro-cracks leading to a higher elastic to viscose proportion until the whole gel breaks resulting in G'' > G'. The frequency sweeps in a range from 10^{-2} to 10^{1} rad/s were performed at low strains. The results proved for the 15 wt% PMEP HG a lower modulus, with G' = $2-10{\cdot}10^{2}$ and G'' = $1-4{\cdot}10^{2}$ Pa, than for both 15 wt% PEG-based hydrogels. Indeed, PEG(4,000) HG exhibited significantly higher values: G' = $4–8{\cdot}10^{3}$ and G'' = $1{\cdot}10^{3}$ Pa. PEG(10,000) HG with longer polymer chains and therefore less crosslinking density has a bit lower moduli compared to PEG(4,000) HG with G' = $2–4{\cdot}10^{3}$ and G'' = $3–15{\cdot}10^{2}$ Pa. The frequency sweeps of 10 wt% HG showed the same trend for all the gels, but with lower elastic and viscous modulus compared to the 15 wt% HG due to the lower crosslinking density. However, in comparison to the PEG-based hydrogels, the 10 wt% PMEP-hydrogel exhibited significantly lower values for both G' = $3–10{\cdot}10^{1}$ Pa and G'' = $1–4{\cdot}10^{1}$ Pa (10 wt% PEG(4,000) HG had G' = $1–2{\cdot}10^{3}$ Pa and G'' = $1–8{\cdot}10^{2}$ Pa; PEG(10,000) HG had G' = $6–15{\cdot}10^{2}$ Pa and G'' = $1–7{\cdot}10^{2}$ Pa). The values of G' at low frequency can be used to make a point about the crosslinking density and the stiffness of different samples. As expected, the hydrogel based on PEG(4,000) exhibited the highest G' value, which means it had the highest stiffness. The PMEP-based hydrogel and the PEG(10,000)-based hydrogel exhibited similar crosslinking density, however, the difference in G' was lower between PEG(4,000) HG and PEG(10,000) HG.

Hydrolytic Degradation. For many biomedical applications such as wound healing dressings, controlled drug release devices, cell immobilization islets, three-dimensional cell culture substrates, and bioactive scaffolds for regenerative medicine the biodegradation of the hydrogel is a preferred or a required property [3,48]. In tissue engineering, degradable hydrogels allow the infiltration of blood vessels and provide space for proliferating cells [49,50]. In controlled drug and gene delivery, degradation permits spatiotemporal controlled release of the cargo [4]. Since the degradability of hydrogels is of importance for many applications, the hydrolysis of the PMEP hydrogels was evaluated and compared to PEG hydrogels. Looking at the chemical structure of the PMEP-hydrogels, both the phosphoesters and the ester bond to the methacrylate at the chain end could be hydrolyzed, while in the PEG gels only the hydrolysis of the methacrylate would lead to degradation of the gel and solubilization of certain degradation products.

The hydrolysis of the hydrogels was studied in DPBS at 37 °C over several weeks. The weight loss of all gels was measured, proving a significantly faster degradation of PMEP hydrogels compared to the PEG-based control samples (Fig. 5a, Tables S1 and S2). PMEP hydrogels exhibited a clear mass loss, which was dependent on the polymer concentration used for the preparation of the hydrogel. After 3 weeks, the 10 wt% PMEP HG was almost completely dissolved. In the case of the 15 wt% PMEP HG, more than 80% weight loss was observed after an incubation time of 6 weeks. In contrast, both PEG hydrogels showed only an initial weight change due to a certain swelling or de-swelling, but did not degrade further under these conditions for at least 5 weeks. The hydrolytic degradation of the PMEP hydrogels was further investigated by ^{31}P NMR spectroscopy, similar to hydrolysis studies we had reported before for PPEs in solution (conducted under neutral conditions (at pH = 7.4 in 0.1 M DPBS buffer/D_2O (9:1)), Fig. 5b) [35]. Following the degradation process over 41 days, an increasing resonance for phosphotriesters at −0.2 ppm due to solubilized polymer fragments, which were released from the network by main-chain hydrolysis, was detected. Besides, an increasing signal at ca. 2 ppm, for phosphodiesters further proved the hydrolysis of PMEP and the degradation of the main-chain (*note*: a constant signal of phosphate of the buffer was visible in all samples).

Cell Adhesion. PEG-based hydrogels are often used in tissue engineering due to their low cell adhesion [51]. To demonstrate the feasibility of using PMEP hydrogels for tissue engineering, the cell adherence was studied. Previously, MG-63 cells were studied on PEG-

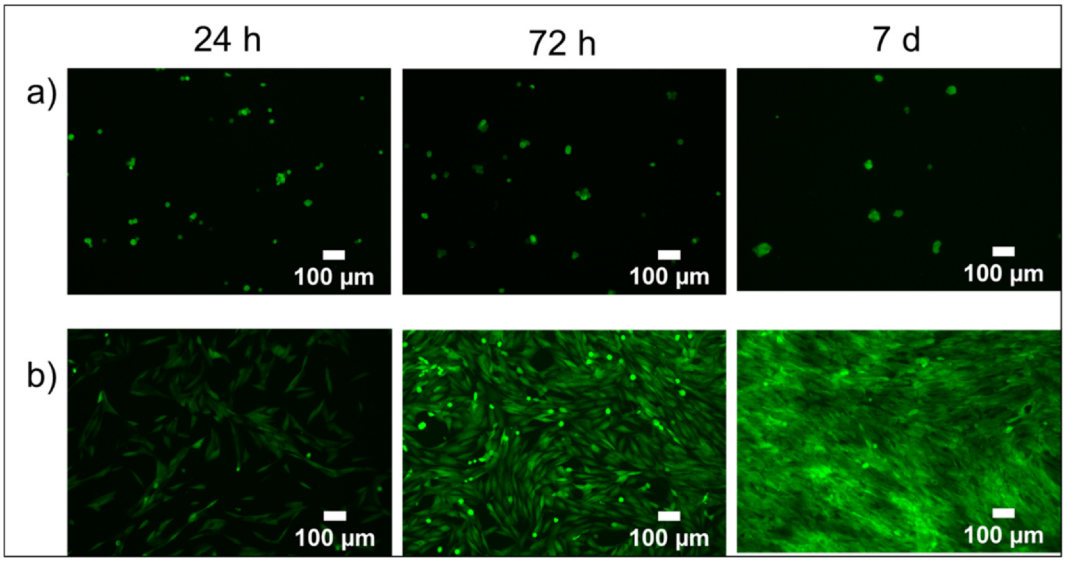

Fig. 6. Cell adherence and viability of the osteoblast cell-line MG-63 over (a) 15 wt% PMEP HGs and (b) seeded into plastic wells of the cell culture plate as a positive control after 24 h, 72 h and 7 days. Viable cells were indicated by green fluorescence with calcein-AM staining.

based hydrogels and a low cell adhesion was detected [52]. To compare the cell adhesion of PMEP-hydrogels, the osteoblast cell line MG-63 were sowed over 15 wt% PMEP HGs (the empty plastic wells were used as a positive control (Fig. 6)). The PMEP hydrogels proved a very low cell adherence during the conducted period while the positive control showed already a significant amount of cells after 24 h. The few cells on the PMEP HGs maintained a round shape and showed no spreading on the gel substrate over time, which indicates non-adherent cells. However, the morphology of cells is dependent on the substrate these cells proliferate and adhere. Hydrogels have usually surface irregularities with small gaps (network mesh) due to the polymer network they form compared to the plain and smooth surface of cell culture plates. Further studies are underway to understand the effect of the surface roughness of PPE-hydrogels and the influence of the phosphate degradation products on the cell growth of osteoblast cell lines.

4. Summary

We prepared polyphosphoester hydrogels based on PMEP homopolymers, which degraded at physiological conditions, and exhibited low cytotoxicity, while being cell-repellent similar as PEG hydrogels. The hydrogels were prepared by the ring-opening polymerization of MEP, followed by end-capping with methacrylates, and crosslinking the PMEP macromonomers under UV-irradiation. Clear, soft, and degradable PMEP hydrogels were obtained. Osteoblasts proved no adhesion to the hydrophilic PMEP, comparable to PEG hydrogels [52], indicating a potential use to prevent postoperative adhesions or thrombosis in damaged blood vessels after angioplasty. Further, these materials might be interesting in controlled drug and gene delivery applications or as scaffolds for regenerative medicine with the integration of adhesion peptides like RGD sequences (Arg-Gly-Asp). Because of the high hydrophilicity of PMEP-MA, it is possible to synthesize polyphosphoester hydrogels without copolymerization of PPEs, which keeps the synthesis effort relatively low, while gaining high control over molar mass and dispersity. However, a combination of PEG and PMEP might be investigated for gels to introduce degradable units together with the known mechanical properties of PEG hydrogels.

CRediT authorship contribution statement

Hisaschi T. Tee: Investigation, Validation, Methodology, Writing - original draft, Writing - review & editing. **Romina Zipp:** Investigation, Methodology, Writing - original draft, Writing - review & editing. **Kaloian Koynov:** . **Wolfgang Tremel:** Supervision, Methodology, Writing - review & editing. **Frederik R. Wurm:** Conceptualization, Project administration, Funding acquisition, Supervision, Writing - review & editing.

Declaration of Competing Interest

The authors declare that they have no known competing financial interests or personal relationships that could have appeared to influence the work reported in this paper.

Acknowledgments

F.R.W. and H.T.T. thank Heraeus Medical (Wehrheim, Germany) for support. We also thank Andreas Hanewald (MPIP) for technical assistance with the rheological measurements.

Data in brief

All raw data will be made available on request.

Appendix A. Supplementary material

Additional characterization data is available (DSC curves, Reverse-phase HPLC assisted determination of the hydrophilicity, HG weights for swelling and degradation, NMR and IR spectra are available). Supplementary data to this article can be found online at https://doi.org/10.1016/j.eurpolymj.2020.110075.

References

[1] N.A. Peppas, J.Z. Hilt, A. Khademhosseini, R. Langer, Hydrogels in biology and medicine: from molecular principles to bionanotechnology, Adv. Mater. 18 (11) (2006) 1345–1360.
[2] A.S. Hoffman, Hydrogels for biomedical applications, Adv. Drug Deliv. Rev. 64 (2012) 18–23.
[3] J.L. Drury, D.J. Mooney, Hydrogels for tissue engineering: scaffold design variables and applications, Biomaterials 24 (24) (2003) 4337–4351.
[4] C.-C. Lin, K.S. Anseth, PEG hydrogels for the controlled release of biomolecules in regenerative medicine, Pharm. Res. 26 (3) (2009) 631–643.
[5] C.R. Nuttelman, M.A. Rice, A.E. Rydholm, C.N. Salinas, D.N. Shah, K.S. Anseth, Macromolecular monomers for the synthesis of hydrogel niches and their application in cell encapsulation and tissue engineering, Prog. Polym. Sci. 33 (2) (2008) 167–179.

[6] B. Reid, M. Gibson, A. Singh, J. Taube, C. Furlong, M. Murcia, J. Elisseeff, PEG hydrogel degradation and the role of the surrounding tissue environment, J. Tissue Eng. Regen. Med. 9 (3) (2015) 315–318.

[7] J.J.F. Verhoef, T.J. Anchordoquy, Questioning the use of PEGylation for drug delivery, Drug Deliv. Translational Res. 3 (6) (2013) 499–503.

[8] K. Knop, R. Hoogenboom, D. Fischer, U.S. Schubert, Poly(ethylene glycol) in drug delivery: pros and cons as well as potential alternatives, Angew. Chem. Int. Ed. 49 (36) (2010) 6288–6308.

[9] A. Basu, K.R. Kunduru, S. Doppalapudi, A.J. Domb, W. Khan, Poly (lactic acid) based hydrogels, Adv. Drug Deliv. Rev. 107 (2016) 192–205.

[10] S.P. Nagam, A.N. Jyothi, J. Poojitha, S. Aruna, R. Nadendla, A comprehensive review on hydrogels, Int. J. Curr. Pharm. Res 8 (1) (2016).

[11] M.N. Mason, A.T. Metters, C.N. Bowman, K.S. Anseth, Predicting controlled-release behavior of degradable PLA-b-PEG-b-PLA hydrogels, Macromolecules 34 (13) (2001) 4630–4635.

[12] A. Goraltchouk, T. Freier, M.S. Shoichet, Synthesis of degradable poly(l-lactide-co-ethylene glycol) porous tubes by liquid–liquid centrifugal casting for use as nerve guidance channels, Biomaterials 26 (36) (2005) 7555–7563.

[13] D.K. Wang, S. Varanasi, E. Strounina, D.J.T. Hill, A.L. Symons, A.K. Whittaker, F. Rasoul, Synthesis and characterization of a POSS-PEG macromonomer and POSS-PEG-PLA hydrogels for periodontal applications, Biomacromolecules 15 (2) (2014) 666–679.

[14] A.T. Metters, K.S. Anseth, C.N. Bowman, Fundamental studies of biodegradable hydrogels as cartilage replacement materials, Biomed. Sci. Instrum. 35 (1999) 33–38.

[15] X. Zhao, J. Milton Harris, Novel degradable poly (ethylene glycol) hydrogels for controlled release of protein, J. Pharm. Sci. 87 (11) (1998) 1450–1458.

[16] K.N. Bauer, H.T. Tee, M.M. Velencoso, F.R. Wurm, Main-chain poly(phosphoester)s: History, syntheses, degradation, bio-and flame-retardant applications, Prog. Polym. Sci. 73 (Supplement C) (2017) 61–122.

[17] T. Steinbach, F.R. Wurm, Poly(phosphoester)s: A new platform for degradable polymers, Angew. Chem. Int. Ed. 54 (2015) 6098–6108.

[18] S. Schöttler, G. Becker, S. Winzen, T. Steinbach, K. Mohr, K. Landfester, V. Mailänder, F.R. Wurm, Protein adsorption is required for stealth effect of poly (ethylene glycol)- and poly(phosphoester)-coated nanocarriers, Nat. Nano 11 (4) (2016) 372–377.

[19] M. Steinmann, M. Wagner, F.R. Wurm, Poly(phosphorodiamidate)s by olefin metathesis polymerization with precise degradation, Chem. – A Eur. J. 22 (2016) 17329–17338.

[20] R.,W.F., Binding matters: binding patterns control the degradation of phosphorus-containing polymers. Green Mater. 2016, 4 (4), 135-139.

[21] J. Beament, T. Wolf, J.C. Markwart, F.R. Wurm, M.D. Jones, A. Buchard, Copolymerization of cyclic phosphonate and lactide: synthetic strategies toward control of amphiphilic microstructure, Macromolecules 52 (3) (2019) 1220–1226.

[22] K.N. Bauer, L. Liu, D. Andrienko, M. Wagner, E.K. Macdonald, M.P. Shaver, F.R. Wurm, Polymerizing phostones: a fast way to in-chain poly(phosphonate)s with adjustable hydrophilicity, Macromolecules 51 (4) (2018) 1272–1279.

[23] T. Wolf, T. Steinbach, F.R. Wurm, A library of well-defined and water-soluble poly (alkyl phosphonate)s with adjustable hydrolysis, Macromolecules 48 (2015) 3853–3863.

[24] L.K. Müller, T. Steinbach, F.R. Wurm, Multifunctional poly(phosphoester)s with two orthogonal protective groups, RSC Adv. 5 (53) (2015) 42881–42888.

[25] T. Steinbach, R. Schroder, S. Ritz, F.R. Wurm, Microstructure analysis of biocompatible phosphoester copolymers, Polym. Chem. 4 (16) (2013) 4469–4479.

[26] R. Riva, U. Shah, J.-M. Thomassin, Z. Yilmaz, A. Lecat, A. Colige, C. Jérôme, Design of degradable polyphosphoester networks with tailor-made stiffness and hydrophilicity as scaffolds for tissue engineering, Biomacromolecules 21 (2) (2020) 349–355.

[27] Q. Li, J. Wang, S. Shahani, D.D.N. Sun, B. Sharma, J.H. Elisseeff, K.W. Leong, Biodegradable and photocrosslinkable polyphosphoester hydrogel, Biomaterials 27 (7) (2006) 1027–1034.

[28] J. He, P. Ni, S. Wang, H. Shao, M. Zhang, X. Zhu, Synthesis and physicochemical characterization of biodegradable and pH-responsive hydrogels based on polyphosphoester for protein delivery, J. Polym. Sci., Part A: Polym. Chem. 48 (9) (2010) 1919–1930.

[29] Z. Liu, L. Wang, C. Bao, X. Li, L. Cao, K. Dai, L. Zhu, Cross-linked PEG via degradable phosphate ester bond: synthesis, water-swelling, and application as drug carrier, Biomacromolecules 12 (6) (2011) 2389–2395.

[30] G. Becker, L.M. Ackermann, E. Schechtel, M. Klapper, W. Tremel, F.R. Wurm, Joining two natural motifs: catechol-containing poly(phosphoester)s, Biomacromolecules 18 (3) (2017) 767–777.

[31] Y. Hao, J. He, X. Ma, L. Feng, M. Zhu, Y. Zhai, Y. Liu, P. Ni, G. Cheng, A fully degradable and photocrosslinked polysaccharide-polyphosphate hydrogel for tissue engineering, Carbohydr. Polym. 225 (2019) 115257.

[32] H. Chen, L. Guo, J. Wicks, C. Ling, X. Zhao, Y. Yan, J. Qi, W. Cui, L. Deng, Quickly promoting angiogenesis by using a DFO-loaded photo-crosslinked gelatin hydrogel for diabetic skin regeneration, J. Mater. Chem. B 4 (21) (2016) 3770–3781.

[33] M. Bessho, M. Furuta, T. Kojima, S. Okuda, M. Hara, Gelatin hydrogels cross-linked by γ-ray irradiation: materials for absorption and release of dye, J. Biomater. Sci. Polym. Ed. 16 (6) (2005) 715–724.

[34] X. Zhao, Q. Lang, L. Yildirimer, Z.Y. Lin, W. Cui, N. Annabi, K.W. Ng, M.R. Dokmeci, A.M. Ghaemmaghami, A. Khademhosseini, Photocrosslinkable gelatin hydrogel for epidermal tissue engineering, Adv. Healthcare Mater. 5 (1) (2016) 108–118.

[35] K.N. Bauer, L. Liu, M. Wagner, D. Andrienko, F.R. Wurm, Mechanistic study on the hydrolytic degradation of polyphosphates, Eur. Polym. J. 108 (2018) 286–294.

[36] M. Schwarzer, T. Otto, M. Schremb, C. Marschelke, H.T. Tee, F.R. Wurm, I.V. Roisman, C. Tropea, A. Synytska, Supercooled water drops do not freeze during impact on hybrid janus particle-based surfaces, Chem. Mater. 31 (1) (2019) 112–123.

[37] R.C. Pratt, B.G.G. Lohmeijer, D.A. Long, P.N.P. Lundberg, A.P. Dove, H. Li, C.G. Wade, R.M. Waymouth, J.L. Hedrick, Exploration, optimization, and application of supramolecular thiourea−amine catalysts for the synthesis of lactide (co) polymers, Macromolecules 39 (23) (2006) 7863–7871.

[38] S.A. Bencherif, A. Srinivasan, J.A. Sheehan, L.M. Walker, C. Gayathri, R. Gil, J.O. Hollinger, K. Matyjaszewski, N.R. Washburn, End-group effects on the properties of PEG-co-PGA hydrogels, Acta Biomater. 5 (6) (2009) 1872–1883.

[39] R. Unger, Q. Huang, K. Peters, D. Protzer, D. Paul, C. Kirkpatrick, Growth of human cells on polyethersulfone (PES) hollow fiber membranes, Biomaterials 26 (14) (2005) 1877–1884.

[40] B. Clément, B. Grignard, L. Koole, C. Jérôme, P. Lecomte, Metal-free strategies for the synthesis of functional and well-defined polyphosphoesters, Macromolecules 45 (11) (2012) 4476–4486.

[41] M. Chen, M. Zhong, J.A. Johnson, Light-controlled radical polymerization: mechanisms, methods, and applications, Chem. Rev. 116 (17) (2016) 10167–10211.

[42] P.-D. Hong, J.-H. Chen, Network structure and chain mobility of freeze-dried polyvinyl chloride/dioxane gels, Polymer 39 (23) (1998) 5809–5817.

[43] Tanaka, T., Gels. Scientific American 1981, 244 (1), 124-36, 138.

[44] J. Simon, T. Wolf, K. Klein, K. Landfester, F.R. Wurm, V. Mailänder, Hydrophilicity regulates the stealth properties of polyphosphoester-coated nanocarriers, Angew. Chem. Int. Ed. 57 (19) (2018) 5548–5553.

[45] A. Engler, H. Sweeney, D. Discher, J.E. Schwarzbauer, Extracellular matrix elasticity directs stem cell differentiation, J. Musculoskelet. Neuronal Interact. 7 (4) (2007) 335.

[46] A.J. Engler, S. Sen, H.L. Sweeney, D.E. Discher, Matrix elasticity directs stem cell lineage specification, Cell 126 (4) (2006) 677–689.

[47] M.L. Oyen, Mechanical characterisation of hydrogel materials, Int. Mater. Rev. 59 (1) (2014) 44–59.

[48] Y. Qiu, K. Park, Environment-sensitive hydrogels for drug delivery, Adv. Drug Deliv. Rev. 53 (3) (2001) 321–339.

[49] J.D. Kretlow, A.G. Mikos, From material to tissue: Biomaterial development, scaffold fabrication, and tissue engineering, AIChE J. 54 (12) (2008) 3048–3067.

[50] E.C. Novosel, C. Kleinhans, P.J. Kluger, Vascularization is the key challenge in tissue engineering, Adv. Drug Deliv. Rev. 63 (4) (2011) 300–311.

[51] J.H. Lee, H.B. Lee, J.D. Andrade, Blood compatibility of polyethylene oxide surfaces, Prog. Polym. Sci. 20 (6) (1995) 1043–1079.

[52] R. Schröder, L. Besch, H. Pohlit, M. Panthöfer, W. Roth, H. Frey, W. Tremel, R.E. Unger, Particles of vaterite, a metastable CaCO3 polymorph, exhibit high biocompatibility for human osteoblasts and endothelial cells and may serve as a biomaterial for rapid bone regeneration, J. Tissue Eng. Regen. Med. 12 (7) (2018) 1754–1768.